Research Square

Preprints are preliminary reports that have not undergone peer review.
They should not be considered conclusive, used to inform clinical practice,
or referenced by the media as validated information.

Topography Shapes Microbial Communities and Functional Potential in Degraded Alpine Meadows

Ziao Liu
Xi'an Jiaotong-Liverpool University
Zheng Chen
Xi'an Jiaotong-Liverpool University
Raj Whitlock
University of Liverpool
Ruoying Zheng
Xi'an Jiaotong-Liverpool University
Xinyue Chen
Xi'an Jiaotong-Liverpool University
Shenghui Weng
Soochow University
Xingyue Qiao
Xi'an Jiaotong-Liverpool University
Xinzhao Tong
Xi'an Jiaotong-Liverpool University
Li Li
li.li01@xjtlu.edu.cn

Xi'an Jiaotong-Liverpool University

Research Article

Keywords:

Posted Date: November 19th, 2026

DOI: https://doi.org/10.21203/rs.3.rs-11553534/v1

License: This work is licensed under a Creative Commons Attribution 4.0 International License.
Read Full License

Additional Declarations: No competing interests reported.

Topography Shapes Microbial Communities and Functional Potential in Degraded Alpine Meadows

Ziao Liu[a,b], Zheng Chen[a], Raj Whitlock[b], Ruoying Zheng[c], Xinyue Chen[c], Shenghui Weng[d], Xingyue Qiao[a], Xinzhao Tong[c*], Li Li[a*]

a. **Centre of Excellence for One Heath and Environmental Sustainability, Academy of Life and Natural Sciences, Xi'an Jiaotong-Liverpool University, Suzhou, 215123, China**

b. **Department of Evolution, Ecology and Behaviour, Institute of Infection, Veterinary and Ecological Sciences, Faculty of Health and Life Sciences, University of Liverpool, Liverpool, L69 3BX, United Kingdom**

c. **Academy of Life and Natural Sciences, Xi'an Jiaotong-Liverpool University, Suzhou, 215123, China**

d. **Jiangsu Key Laboratory of Infection and Immunity, Institutes of Biology and Medical Sciences, Soochow University, Suzhou 215123, China**

***Corresponding authors (Li Li, email: li.li01@xjtlu.edu.cn; telephone number: +86 (0)512 8188 8373 Xinzhao Tong, email: xinzhao.tong@xjtlu.edu.cn; telephone number: 86-512-88161650)**

Abstract

Grassland desertification on the Qinghai-Tibetan Plateau (QTP) strongly alters alpine meadow ecosystems, but the relative roles of topography, and soil water availability in shaping microbial communities along desertification gradient remain unclear. We performed shotgun metagenomic sequencing of degraded alpine meadow soils and investigated microbial taxonomic and targeted functional responses across desertification stages and topographic positions. Environmental variation was primarily structured by soil water content (SWC) and variables related to nutrients. The first principal component explained 66.4% of environmental variation. SWC differed significantly between topographic positions ((F = 43.17, $p < 0.001$)) but not with degradation stages (F = 2.34, p = 0.106). PERMANOVA showed significant effects of topography on both genus ($R^2 = 0.118$, p = 0.043) and targeted functional composition ($R^2 = 0.119$, p = 0.031). dbRDA identified SWC as the strongest environmental gradient, whereas variation partitioning analysis indicated larger shared environmental effects for targeted functional profiles (54.6%) and stronger independent soil property effects for genus composition (15.1%). β-diversity was dominated by turnover at both genus (83.5%) and targeted functional (72.5%) levels. These results suggest that topography indirectly shapes microbial community assembly through environmental heterogeneity and that taxonomic and functional responses show partial coupling across alpine meadow soils impacted by desertification.

Keywords

Grassland degradation; soil water content; topography; soil microbiome; microbial community assembly; functional redundancy; beta diversity

Statements and Declarations

Competing Interests

The authors declare that they have no competing interests that are relevant to the content of this article.

Funding

This work was supported by the National Natural Science Foundation of China - Young Scientist Fund (42101098).

Introduction

Terrestrial ecosystems regulate global carbon storage, nutrient cycling, and biodiversity (Chapin Iii et al., 2000). However, widespread ecosystem degradation driven by intensive land use and climate change has affected more than one-third of the global land area and led to substantial losses in ecosystem functioning and stability (Ellis, 2011; Intergovernmental Panel On Climate Change (Ipcc), 2023).

Soil microbial communities are central regulators of ecosystem responses to environmental degradation (Bardgett and Van Der Putten, 2014; Fierer, 2017). They control carbon decomposition and nitrogen cycling, and strongly influence ecosystem stability. In forest ecosystems under logging and land-use intensification, long-term reductions in soil carbon following disturbance are driven by changes in substrate availability and decomposition processes mediated by microbes (Bowd et al., 2019) . In permafrost ecosystems, warming-induced thawing alters microbial community structure, shifting it from slow-growing, carbon-sequestrating taxa toward fast-growing carbon decomposers. This transition alters microbial function and accelerates the breakdown of frozen organic matter, which leads to increased carbon release and strengthening climate feedbacks (Schuur et al., 2015). Among these systems, degradation alters microbial community structure and function through changes in resource availability and environmental constraints. These microbial shifts, in turn, affect soil nutrient cycling by altering the rate of carbon decomposition and nitrogen transformation, thereby influencing ecosystem degradation trajectories. In different forms of degradation, water availability is always a key limiting factor for microbial activity. SWC reflects the combined influence of multiple environmental variables and shapes microbial processes and community assembly (Schimel, 2018).

Building on its role as a key limiting factor for microbial activity, the regulatory effects of SWC are reflected in both community composition and functional processes. Changes in soil moisture regulate microbial processes through multiple interconnected

mechanisms. At low SWC in dryland and semi-arid soil systems, reduced water films and increased pore discontinuity restrict substrate diffusion and microbial mobility, limiting access to organic carbon and nutrients. This physical constraint suppresses microbial activity and enzyme activity, ultimately slowing carbon decomposition and nutrient cycling (Tecon and Or, 2017). Declining moisture also reshapes soil microbial community composition by favoring drought-tolerant taxa and reducing the abundance of fast-growing and resource-demanding groups (Canarini et al., 2021). These community shifts are accompanied by changes in microbial metabolic efficiency, leading to reduced carbon-use efficiency and altered decomposition pathways. SWC is not only a major constraint on microbial activity, but also a central regulator of ecosystem functioning and degradation dynamics (Delaux et al., 2013; Schimel, 2018). It links climatic variability with belowground ecological processes by regulating plant productivity, root carbon inputs, nutrient diffusion, and microbial metabolism (Sokol et al., 2022; Tecon and Or, 2017). Declining SWC is closely associated with land degradation processes, particularly desertification. Reduced soil moisture weakens soil aggregation and increases erosion risk, leading to nutrient loss and reduced soil stability (Berdugo et al., 2020; D'Odorico et al., 2013). At the plant community level, water limitation constrains plant growth and accelerates vegetation loss, further reducing soil protection and water retention capacity. For example, in the semi-arid woodland ecosystem of southwestern North America, persistent drought led to widespread mortality of *Pinus edulis*, resulting in abrupt vegetation loss and increased soil erosion (Breshears et al., 2005). Similarly, in temperate semi-arid grassland ecosystems, reduced precipitation significantly decreases aboveground biomass and plant cover, weakening soil stabilization and increasing desertification risk (Knapp et al., 2008). Therefore, SWC may act as a key driver of in regulating ecosystem processes across spatial scales, linking climate change with plant soil–microbial interactions in desertifying terrestrial systems.

The QTP is one of the largest alpine ecosystems in the world and plays an important

role in regional and global carbon storage, hydrological regulation, and climate regulation. Soil organic carbon (SOC) storage in the QTP amounts to 18 Pg, accounts for 1.22% of the global terrestrial SOC pool (Tian et al., 2008). Alpine meadows on the QTP are shaped by harsh environmental conditions, including cold temperatures, strong radiation, and high environmental sensitivity, with water availability acting the primary limiting factor in the desertification process (Harris, 2010). In recent decades, over 70% of the QTP's grassland have undergone varying degrees of degradation (NDRC, 2020), driven by combined effects of climate change such as atmospheric warming and altered precipitation regimes, and human activities like overgrazing (Harris, 2010; Li et al., 2017). Alpine meadows on the QTP are dominated by *Kobresia pygmaea*, which is characterized by low-stature vegetation, dense turf structure, and high belowground biomass allocation (Miehe et al., 2019). These characteristics provide strong soil stabilization and carbon storage capacity. During the desertification process, native intact Kobresia turf layer becomes fragmented and eventually stripped, leading to the loss of the sod layer. This transition is typically accompanied by the invasion and expansion of less palatable weeds, replacing the original vegetation community and further reducing ecosystem stability (Dong et al., 2023). As a result, soil exposure increases, SOC is lost more rapidly, and ecosystem functions decline. Given that QTP grasslands constitute a key component of the Asian water tower and a major terrestrial carbon sink, the degradation of the QTP grassland has implications beyond the regional scale. It affects hydrological regulation and other ecosystem services in the downstream regions, and influences global carbon cycling and climate feedback. These processes highlight the sensitivity of alpine grassland ecosystems on the QTP, particularly to changing hydroclimatic conditions associated with global climate change (Lehnert et al., 2016).

Topography is another central factor in the desertification on the QTP, and it also strongly influences grassland restoration. It controls SWC redistribution and microenvironmental heterogeneity, thereby shaping vegetation establishment, nutrient

availability, and microbial habitat conditions (Dai et al., 2023; Li et al., 2024). In alpine grasslands, sloping habitats often experience lower soil moisture levels, more intense runoff, and higher erosion intensity than flat-plain areas. These differences can further affect plant growth and microbial activity because soil microorganisms are highly sensitive to water availability. Previous studies have shown that microtopographic variation significantly alters microbial community composition and functional guilds in alpine meadow on the QTP (Li et al., 2024). Similarly, slope aspect has been reported to influence plant biomass, soil properties, and microbial composition in alpine meadows through regulating soil moisture and microclimate (Xue et al., 2018). Studies have shown that vegetation recovery on desertified slopes is challenging, as ongoing erosion and water loss progressively reduce soil stability and water retention capacity (Qian et al., 2024). Therefore, understanding the role of topographic heterogeneity is essential for explaining microbial dynamics and ecosystem functioning during grassland degradation and restoration on the QTP.

Recent studies have shown that grassland desertification the QTP alters soil microbial community composition and functional potential. For example, metagenomic analyses indicate significant shifts in microbial taxa and carbon metabolism during Kobresia turf loss, which are closely associated with changes in soil properties (Wu et al., 2024). In addition, slope position has been shown to significantly influence microbial community structure, highlighting the role of topography in shaping microbial heterogeneity (Li et al., 2024). Soil moisture has also been identified as a dominant environmental driver controlling microbial assembly and ecosystem processes across QTP ecosystems (Yang et al., 2023). Despite increasing recognition that SWC, topography, and loss of the sedge turf jointly influence soil microbial communities, most studies have examined these factors separately rather than within a unified framework. In particular, how SWC interacts with grassland degradation gradients and topographic variation to shape microbial community structure and functional composition remains unclear. Moreover, the relationship between taxonomic shifts and functional potential across

environmental gradients is still not well resolved in the QTP alpine meadow ecosystems.

In this study, we used shotgun metagenomic sequencing to investigate how SWC and environmental heterogeneity associated with desertification gradients and topographic variation shape soil microbial community diversity, composition, and functional potential in alpine meadow ecosystems on the QTP. We integrated taxonomic and functional analyses to evaluate the relative importance of SWC, degradation gradients, and topography in driving microbial diversity patterns and functional shifts.

We hypothesized that: (1) SWC is a primary driver of microbial community assembly and functional variation across grassland desertification gradients; (2) Topography controls microbial diversity and composition by altering environmental conditions; (3) Microbial taxonomic shifts are closely coupled with changes in functional potential along environmental gradients on the QTP.

Methods & Materials

Study system

This study was conducted in alpine meadows located in Jiuzhi County, Guoluo Tibetan Autonomous Prefecture, Qinghai Province, China (33°25′45″N, 101°28′58″E; Figure 1). The study region is situated on the southeastern QTP at elevation above 4000 m, with a mean annual temperature of approximately 0.1°C and mean annual precipitation of about 760 mm (Han, 2015). To investigate microbial responses to alpine grassland desertification, sampling sites were established across a complete degradation gradient, including 6 stages. Degradation stages were classified according to the proportion of barren patch area within 1 m×1 m quadrats. Specifically, stage 1 represented native intact alpine meadow without visible barren patches, while stage 2-6 corresponded to bare-soil patch coverage of 5-20%, 20%-40%, 40%-60%, 60%-80%, and >80%, respectively. To further assess the influence of topographic heterogeneity, both slope and flat sites were included with each degradation stage. The slope sites were

characterized by greater surface runoff and lower soil water retention, whereas flat sites generally maintained relatively higher soil moisture and vegetation cover.

Field survey and Sampling

Field sampling was conducted during the plant growing season in June 2022. A total of 48 soil samples were sequenced, and paired upper-lower soil samples from the same sampling location were averaged prior to downstream analyses. All samples were collected from the same pasture to minimize large-scale environmental variation among sites and ensure that all sampling sites were subjected to relatively similar grazing pressure. Both slope and flat plain were included, with 12 samples collected from each topography type. Soil samples distribution was listed in Table S1. Within each topographic position, two replicate samples were collected for each degradation stage. A minimum distance of 10 m was maintained between sampling plots to reduce potential spatial dependence among samples. This sampling design allowed us to evaluate the effects of desertification and topographic heterogeneity on soil microbial community composition and functional potential. It also minimized potential confounding effects associated with grazing management and large-scale environmental variation. At each site, soil samples were collected using a 4 cm diameter soil core sampler, extracting 0-10 cm topsoil samples at each designated sampling point. All soil samples were stored at -20°C until they were sent to laboratory.

Laboratory soil processing and analysis

Soil samples were homogenized and passed through a 2 mm sieve to remove visible roots, stones, and plant debris. 1 g of fresh soil was weighed and stored at −80°C for subsequent DNA extraction and metagenomic analysis. The remaining soil was air-dried at room temperature for physicochemical analyses. For chemical measurements, air-dried soil samples were further finely ground in an agate mortar and sieved through a 0.125 mm mesh. Total carbon (TC) and total nitrogen (TN) contents were determined

using an elemental analyzer (Thermo Fisher, China). Dissolved organic carbon (DOC) and dissolved nitrogen (DN) were determined using a TOC/TN analyzer (Analytik Jena, Germany). Soil organic matter (SOM) was determined using the loss on ignition method at 550 °C (Ghabbour et al., 2014). SWC was determined using a gravimetric method. Approximately 2 g of fresh soil was weighed, wrapped in aluminium foil, and oven-dried at 105 °C till to constant weight. The dried samples were then weighed, and SWC was calculated from the mass of water lost during drying relative to the fresh soil mass. Bulk density (BD) was determined using the core method. To evaluate the relationships among the measured environmental variables and assess the degree of covariance among potential explanatory variables, Pearson correlation coefficients were calculated for SWC, SOM, TN, TC, pH, and BD. Correlation coefficients and associated P values were calculated using the cor.test function in R. The correlation matrix is provided in Table S2.

Shotgun metagenome sequencing, processing, and data analysis

Soil samples were subjected to metagenomic sequencing to characterize microbial taxonomic composition and functional potential. Genomic DNA extraction, library preparation, and sequencing were performed by Logic (Shenzhen) Information Technology Co., Ltd. (Shenzhen, China) following standardized procedures. Genomic DNA was extracted and purified following standard quality control procedures prior to library construction. Sequencing libraries were generated using the DNBSEQ-T7 library preparation kit according to the manufacturer's protocol. Paired-end sequencing was performed on the BGISeq-T7 platform, targeting 15 Gbp of raw data per sample. Sequencing quality was evaluated using predefined criteria to ensure consistency among samples. Data quality standards included paired-end 150 bp reads (PE150) with an average Q20 > 90% and Q30 > 85%. A total of 48 metagenomic samples passing quality requirements were retained for downstream analyses. Raw sequencing reads were subjected to quality filtering and host contamination removal using KneadData,

with the human hg37 database as the reference. The clean sequences were subjected for taxonomic classification using Kraken2, which assigned sequencing reads based on taxonomic similarity and generated microbial abundance profiles at multiple taxonomic levels (Wood et al., 2019). Functional annotation was conducted using HMP Unified Metabolic Analysis Network (HUMAnN 3.0) (Beghini et al., 2021). Sequencing reads were mapped to pangenome-level gene families and metabolic pathways to estimate microbial functional potential. Functional profiling generated gene family abundance tables, pathway abundance matrices, and pathway coverage matrices. To improve biological interpretability and facilitate ecological analysis, UniRef-based gene families were converted into KEGG Orthology (KO) identifiers (Kanehisa, 2000). Functional profiles were subsequently curated by retaining only targeted genes and pathways associated with essential ecological processes relevant to this study, including carbon cycling, nitrogen cycling, water-stress responses, and environmental stress adaptation. All other functional categories were excluded from subsequent analyses. For pathway-level analyses, taxonomic stratification information was removed to focus on community-level functional characteristics rather than species-specific contributions.

Statistical analysis

All statistical analyses were performed in R (4.5.1). Prior to analysis, microbial abundance tables were normalized to relative abundance. Differences in SWC among degradation stages were evaluated using the Kruskal-Wallis test (Kruskal and Wallis, 1952). Post hoc pairwise comparisons were performed using Dunn's test with Benjamini-Hochberg (BH) correction for multiple comparisons (Dunn, 1964). Differences in SWC between topographies were assessed using the Wilcoxon rank sum test (Wilcoxon, 1945). These analyses were conducted using the packages rstatix (version 0.7.3) and FSA (version 0.10.1) in R. To test whether the relationship between topographic position and SWC varied across degradation stages, I fitted a two-way linear model with degradation stage, topographic position, and their interaction as

explanatory terms. Degradation stage and topographic position were treated as categorical variables. The significance of the main effects and their interaction was evaluated using analysis of variance (ANOVA) (Table S3). Principal component analysis (PCA) was conducted using the prcomp function in the base stats (version 4.5.1) package. It was used for dimensionality reduction of environmental variables, and the resulting ordination scores were used to visualize variation across degradation stages and topography. The analysis was based on soil physicochemical variables, including SWC, BD, pH, TC, TN, SOM, DOC, DN, root biomass, and carbon stock.

Alpha diversity indices, including Shannon, Simpson, and Richness, were calculated at the genus level using the vegan (version 2.7.3) package. Non-metric multidimensional scaling (NMDS) based on Bray-Curtis dissimilarity was performed using the metaMDS function in the vegan package to evaluate differences in microbial community composition and the targeted subset of KEGG orthologs among degradation stages and topographic positions (Oksanen et al., 2001). NMDS ordination was performed with two dimensions (k = 2) and 100 random strats (trymax = 100) to improve stability. The environmental fitting analysis was subsequently conducted using the envfit function in vegan with 999 permutations to assess relationships between microbial community structure and environmental variables, including SWC, TN, TC, pH, and BD. (Oksanen et al., 2001). Permutational multivariate analysis of variance (PERMANOVA) was performed using the adonis2 function in the vegan (version 2,7,3) package to evaluate whether microbial taxonomic and targeted KEGG functional composition were affected by SWC, degradation, and topography (Anderson, 2001). The analysis was based on Bray-Curtis dissimilarity matrices:

$$d_{BC} = 1 - \frac{2C_{ij}}{S_i + S_j}$$

Where C_{ij} is the sum of shared abundances between samples i and j. S_i and S_j are total abundances.

Marginal effects of individual variables were assessed using the by = "margin" option with 999 permutations. Homogeneity of multivariate dispersion among degradation levels was tested using the betadisper function, followed by a permutation-based ANOVA.

To further assess the relationships between environmental factors and microbial taxonomic and targeted functional composition, distance-based redundancy analysis (dbRDA) was conducted using the capscale function in the vegan package (Legendre and Anderson, 1999). This analysis quantified the contribution of environmental variables to variation in microbial taxonomic and targeted functional composition across degradation gradients and topographic positions. Variation partitioning analysis (VPA) was performed using the varpart function in the vegan package to quantify the relative contributions of SWC, degradation gradients, and topographic variation on microbial community and targeted functional variation (Legendre, 2008). Taxonomic and functional turnover were assessed based on changes in the relative abundances of dominant genera and targeted KEGG orthologs. This approach identified taxa and genes showing consistent enrichment or depletion along environmental gradients. It provided complementary information on compositional and functional changes beyond ordination-based analyses (Anderson et al., 2011; Legendre and De Cáceres, 2013).

Beta diversity was further decomposed into turnover and nestedness components using the package betapart (version 1.6.1). Bray-Curtis dissimilarity matrices were partitioned using the beta. pair. abund function (Baselga, 2010a, 2013). Turnover represented species or functional replacement among the samples. Nestedness represented richness differences without replacement. The relative contribution of each component was calculated as a proportion of total beta diversity. Analyses were conducted for both taxonomic (genus level) and targeted functional (KEGG ortholog) datasets. Turnover and nestedness components were further compared across SWC gradients and between topographic types (Slope vs Flatplain) to evaluate how

hydrological variation and topography influence microbial community assembly processes.

Heatmaps were constructed to visualize microbial taxa and selected functional genes associated with SWC. Genus-level abundance data and selected functional gene profiles were standardized using Z-score transformation before visualization. Samples were ordered along the SWC gradient from low to high values. Spearman correlation analysis was performed between genus abundance and SWC. The top 20 genera with the strongest absolute correlation coefficients were selected for visualization. Correlation coefficients (rho) and false discovery rate (FDR) adjusted P values were calculated for each genus (Benjamini and Hochberg, 1995). Functional genes involved in carbon, nitrogen cycling, and environmental stress responses were selected for the targeted functional heatmap. Heatmaps were generated using the package pheatmap (version 1.0.13) (Kolde, 2010). Row clustering was applied using hierarchical clustering, whereas column clustering was disabled to preserve the SWC gradient order. Color gradients represented standardized relative abundance values.

Heatmaps of the top 20 dominant genera, SWC-associated taxa, and KEGG functional genes were generated using the package pheatmap (version 1.0.13). SWC-associated taxa were identified based on Spearman correlation analysis between SWC and genus relative abundance, with significance determined at $p < 0.05$ after BH correction.

All figures were generated using the ggplot2 (version 4.0.3) package unless otherwise specified. Statistical significance was determined at $p < 0.05$.

Results

Environmental variation across degradation stages and topographic positions

To characterize variation in soil environmental conditions across degradation stages and topographic positions, PCA was performed using measured soil variables. The first two

principal components explained 82.8% of total environmental variation, with PC1 accounting for 66.4% and PC2 accounting for 16.4% (Table 1). PC1 showed strong negative loadings for TC (−0.384), TN (-0.380), SOM (-0.381), SWC (-0.369), and Carbon Stock (-0.362), and a positive loading for BD (0.319), indicating a dominant environmental gradient associated with soil resource availability and soil physical conditions. PC2 was primarily associated with Root Biomass (-0.667), DN (0.592) and DOC (−0.414), indicating an additional environmental gradient associated with dissolved nutrient availability and belowground biomass. Sample distributions showed structured patterns across degradation stages and topographic positions. Samples from different degradation stages occupied different regions along PC1, whereas intermediate stages exhibited partial overlap (Figure 2A). Topographic groups also showed separation along the principal axes, with slope and flat-plain samples distributed across partially distinct regions of the ordination space. The distribution of environmental loadings and samples indicates that variation in soil water availability, nutrient status, soil physical conditions, belowground biomass, and dissolved nutrient characteristics represented the major environmental gradients across degradation stages and topographic positions.

Pearson correlation analysis showed strong associations among several soil physicochemical properties (Table S2). SWC was strongly positively correlated with SOM ($r = 0.923$, $p < 0.001$), TN ($r = 0.931$, $p < 0.001$), and TC ($r = 0.947$, $p < 0.001$), and negatively correlated with bulk density ($r = -0.872$, $p < 0.001$). SOM, TN, and TC were also strongly correlated with each other, with correlation coefficients ranging from 0.970 to 0.991 ($p < 0.001$). In contrast, correlations involving pH were weaker, although significant positive correlations were observed between pH and SWC, SOM, TN, and TC ($r = 0.543–0.578$, $p < 0.01$). The correlation between pH and bulk density was not statistically significant ($r = -0.403$, $p = 0.051$). Overall, these results indicate that SWC, soil carbon and nitrogen variables, and bulk density were strongly coupled within the measured soil physicochemical gradient.

SWC differed significantly between topographic positions (Wilcoxon test, $p = 2.01 \times 10^{-4}$), with flat-plain sites exhibiting higher SWC values than slope sites (Figure 2C). In contrast, SWC did not show significant variation across degradation stages (Kruskal–Wallis test, $p = 0.489$), although variability among stages was observed (Figure 2B). The observed distribution pattern indicates that variation in SWC was more strongly associated with topographic position than with degradation stage across the sampled sites. A two-way linear model showed that topographic position was significantly associated with SWC ($F = 43.17$, $p < 0.001$), whereas degradation stage was not significant ($F = 2.34$, $p = 0.106$). The degradation stage × topographic position interaction was also not significant ($F = 1.37$, $p = 0.302$), indicating that the difference in SWC between topographic positions did not vary significantly across degradation stages (Table S3).

Genus-level microbial alpha diversity across degradation stages

Genus-level microbial alpha diversity did not differ significantly across degradation stages (Figure S1). Shannon diversity showed no significant variation among stages ($\chi^2 = 0.36$, $p = 0.996$). Similar patterns were observed for richness ($\chi^2 = 1.53$, $p = 0.909$) and Simpson diversity ($\chi^2 = 0.58$, $p = 0.989$). The distributions of all three indices substantially overlapped across degradation stages, indicating limited variation in genus-level microbial diversity along the degradation gradient.

Taxonomic and functional compositional variation across degradation stages and topographic positions

NMDS was used to characterize variation in genus-level microbial community composition across degradation stages and topographic positions. The NMDS ordination produced a low stress value (stress = 0.074), indicating that the two-dimensional configuration adequately represented community dissimilarity patterns. Environmental fitting analysis showed that all measured environmental variables were

significantly associated with microbial community composition (envfit, $p = 0.001$; Table S4). Among these variables, TN showed the highest association with community variation ($r^2 = 0.703$), followed by TC ($r^2 = 0.684$), SOM ($r^2 = 0.677$), and SWC ($r^2 = 0.644$). pH ($r^2 = 0.591$) and BD ($r^2 = 0.508$) also showed significant associations with microbial composition. Environmental vectors of SWC, SOM, TN, and TC were oriented toward similar directions along the positive region of NMDS1 and NMDS2, whereas BD exhibited an opposite directional pattern (Figure 3). Sample distributions showed partial overlap among degradation stages, while flat, plain, and slope samples occupied partially distinct regions of the ordination space. These results indicate that genus-level microbial community variation was associated with coordinated gradients of soil moisture and soil resource variables.

PERMANOVA was performed to evaluate the effects of degradation stage, topographic position, and SWC on microbial taxonomic and targeted functional composition (Table 2). For genus-level microbial composition, the overall model explained 46.6% of community variation ($R^2 = 0.466$, $p = 0.036$). Topography showed a significant association with microbial taxonomic composition ($R^2 = 0.118$, $p = 0.043$), whereas degradation stage ($R^2 = 0.234$, $p = 0.194$) and SWC ($R^2 = 0.035$, $p = 0.373$) did not. Similar patterns were observed for targeted functional composition based on KO profiles. The overall model explained 46.7% of functional variation ($R^2 = 0.467$, $p = 0.043$). Topography showed a significant association with functional composition ($R^2 = 0.119$, $p = 0.031$), whereas degradation stage ($R^2 = 0.229$, $p = 0.192$) and SWC ($R^2 = 0.035$, $p = 0.360$) were not significant. The proportions of explained variation and significance patterns were highly similar between genus-level and targeted functional composition, indicating comparable responses of microbial taxonomic and functional structures across environmental gradients. Multivariate dispersion tests were not significant for either genus-level composition ($p = 0.706$) or targeted functional composition ($p = 0.709$), indicating that the PERMANOVA result was homogeneous within the group.

Overall, the NMDS and PERMANOVA results indicate that microbial taxonomic and targeted functional composition exhibited similar compositional patterns across environmental gradients. Topography showed stronger associations with both datasets than the degradation stage and SWC.

Environmental drivers of microbial taxonomic and functional composition

To quantify the relative contributions of environmental variables to microbial taxonomic and functional variation, dbRDA was performed using SWC, SOM, and TN as explanatory variables. Environmental variables explained substantial proportions of variation in both microbial taxonomic and targeted functional composition. The constrained fraction accounted for 40.2% of total variation in genus-level composition and 39.6% in targeted KO functional composition, whereas the unconstrained fraction accounted for 59.8% and 60.4%, respectively (Figure 4). The overall dbRDA models were significant for both genus-level composition ($F = 4.48$, $p = 0.001$) and KO functional composition ($F = 4.36$, $p = 0.002$) (Table S5), indicating that environmental factors structure microbial communities. The first dbRDA axis explained 30.4% of constrained variation in both datasets, whereas the second axis explained 8.7% and 7.7% of variation in genus-level and KO composition, respectively. Samples showed directional separation along the environmental gradients, indicating consistent associations between microbial composition and environmental variables. Among the measured environmental variables, SWC exhibited the greatest explanatory power for both microbial functional and taxonomic composition. SWC showed significant effects in the KO model ($F = 9.38$, $p = 0.002$) and genus model ($F = 9.88$, $p = 0.001$). TN showed a significant association with functional composition ($F = 2.96$, $p = 0.043$) but not with genus-level composition ($F = 1.98$, $p = 0.127$). SOM did not show significant effects in either model ($p > 0.05$) (Table S5). The longer vector length of SWC relative to SOM and TN further indicated stronger associations with both microbial taxonomic and functional composition. Similar orientations of environmental vectors between

taxonomic and functional ordinations suggested a shared primary environmental gradient associated with soil water availability.

VPA was performed to quantify the relative contributions of SWC, soil properties, and structural factors (degradation stage and topography) to microbial taxonomic and targeted functional composition (Figure 5; Table 3). Environmental variables collectively explained 67.6% of the variation in targeted functional composition and 56.5% of the variation in genus-level composition. For targeted functional composition, the largest proportion of explained variation was attributed to shared effects among environmental components (54.6%), whereas the independent contributions of SWC and soil properties approached zero after adjustment. Structural factors contributed 2.7% of the independent variation. Residual unexplained variation accounted for 32.4%. For genus-level composition, soil properties showed the largest independent contribution (15.1%), followed by structural factors (2.5%) and SWC (1.3%). Shared environmental effects accounted for 19.5% of the explained variation, whereas residual variation accounted for 43.5% of the total community variation. The proportion of shared environmental effects was larger for targeted functional composition than for genus-level composition, whereas the independent contribution of soil properties was greater for microbial taxonomic composition.

Collectively, dbRDA and VPA showed different contributions of environmental components to microbial taxonomic and functional composition. Functional composition showed larger shared environmental effects. Taxonomic composition showed a stronger independent contribution from soil properties.

Turnover-dominated β-diversity in taxonomic and targeted functional profiles

Microbial β-diversity was mainly explained by turnover at both genus and targeted KO levels (Figure S2). At the genus level, turnover accounted for 83.5% of total β-diversity (0.0545), whereas nestedness contributed 16.5% (0.0108). Similar patterns were

observed at the targeted KO level, where turnover accounted for 72.5% of total β-diversity (0.0668) and nestedness accounted for 27.5% (0.0254). Total β-diversity was higher for targeted functional profiles (0.0922) than for genus-level composition (0.0653). Relationships between SWC distance and β-diversity components were evaluated using linear regression (Figure S2A, B, D, and E; Table S6). SWC distance showed no significant relationship with genus-level turnover ($R^2 = 0.0027$, $p = 0.391$) or KO-level turnover ($R^2 = 0.0048$, $p= 0.253$). Regression slopes for turnover remained close to zero across the SWC gradient. Genus-level nestedness showed a significant positive relationship with SWC distance ($R^2 = 0.0264$, $p = 0.0069$), although the explained variation was low. No significant relationship was detected between SWC distance and nestedness of KO level ($R^2 = 0.0003$, $P = 0.763$). Pairwise comparisons among flatplain–flatplain, slope–flatplain, and slope–slope groups showed substantial overlap in turnover values at both genus and targeted KO levels (Figure S2C, F). No clear separation among topographic pair groups was observed. Overall, turnover represented the dominant component of microbial β-diversity at both taxonomic and targeted functional levels. SWC distance showed limited explanatory power for β-diversity patterns.

Taxonomic and functional features across environmental gradients

The top 20 SWC-associated taxa showed strong positive correlations with SWC, with Spearman rho values ranging from 0.74 to 0.83 and FDR values below 0.01 (Figure 6A). *Faecalicatena* showed the strongest correlation with SWC (rho = 0.83, FDR = 0.0019), followed by *Methanomassiliicoccus* and *Novisyntrophococcus* (rho = 0.81, FDR = 0.0019). Other taxa, including *Usitatibacter*, *Hawkeyevirus*, *Cafeteriavirus*, *Methylovulum*, *Anaerolinea*, and *Lacrimispora*, also showed strong positive associations with SWC. Higher standardized abundance values were generally observed in samples with relatively higher SWC values. Targeted functional genes showed heterogeneous abundance patterns across samples and functional categories

(Figure 6B). Genes related to carbon, nitrogen cycling, and stress resistance displayed variable abundance profiles among samples. No consistent monotonic trend was observed along the SWC gradient. Differences in abundance patterns were observed between topographic groups, with subsets of genes showing higher abundance in one group than the other. Variation across degradation stages showed less consistent patterns.

Discussion

Topography may represent a stronger local filter than degradation stage for SWC

Our results suggest that topography was a stronger local correlate than the nominal degradation stage: SWC differed significantly between slope and flat-plain sites, but did not vary significantly among degradation stages (Figure 2C). PERMANOVA also showed significant topographic effects on both genus-level and targeted KO composition, whereas the degradation stage was not significant in either dataset (Table 2). This pattern suggests that the six degradation classes did not fully represent the microbial habitat conditions experienced at the sampling scale. In alpine meadows, microtopography can reshape soil moisture, nutrient redistribution, and microbial habitats. A recent study of alpine meadows in the QTP showed that microtopographic variation affected soil microbial communities by changing soil physicochemical conditions, including moisture and nutrients (Li et al., 2024). This finding aligns well with our results. Slope sites are more likely to experience runoff, erosion, and reduced water retention. Flat-plain sites are more likely to accumulate water and fine soil particles. These processes can create stable differences in microbial habitats even within the same degradation class. This may explain why topography showed clearer statistical effects than desertification at the sampled scale. Similar patterns have been reported at broader scales. Fierer and Jackson showed that soil bacterial diversity was more closely associated with soil variables than with broad geographic categories (Fierer and Jackson, 2006). Our results extend this idea to desertified alpine meadow soils. Topographic

variation can also regulate runoff, soil erosion, and water redistribution, which subsequently influence landscape-scale vegetation fragmentation and patch connectivity during desertification. Zhang et al. reported that terrain conditions significantly affected the spatial expansion of degraded black-soil patches on the QTP (Zhang et al., 2024). These processes may further alter microbial habitats by reshaping local soil moisture and nutrient distribution. Landscape metrics measured at local scales and associated with patch structure and connectivity may therefore reflect environmental heterogeneity linked to microbial variation.

SWC is an important gradient, but its effect is coupled with soil resources

SWC was strongly associated with microbial composition in NMDS and dbRDA analyses (Figure 3; Table S5). The top 20 taxa associated with SWC showed high positive correlations with water content, with rho values ranging from 0.74 to 0.83 (Figure 6). These results support the role of soil water as an important environmental gradient in degraded alpine meadow soils. Soil moisture controls liquid diffusion, oxygen diffusion, substrate access, and microbial metabolic activity. Brockett et al. reported that soil moisture was a major factor associated with microbial community structure and enzyme activities across forest soils in western Canada (Brockett et al., 2012). Banerjee et al. further showed that soil moisture strongly affected microbial community structure and nitrogen-related emissions (Banerjee et al., 2016). However, the association between SWC and microbial composition should be interpreted in the context of the strong covariance among soil physicochemical properties. Correlation analysis showed that SWC was strongly correlated with SOM, TN, TC, and Bulk Density. PCA further showed that SWC clustered with TC, TN, and SOM along the main environmental axis (Figure 2; Table 1). Together, these results indicate that SWC was closely coupled with the broader soil physicochemical gradient rather than representing an isolated environmental condition. We therefore interpret SWC as an important component of this coupled environmental gradient, rather than as an

560 independent driver of microbial composition.

561 However, VPA showed that the independent fraction explained by SWC was low after
562 adjustment, whereas the shared environmental fraction was high, especially for targeted
563 KO profiles (Figure 5; Table 3). This pattern further supports the interpretation that the
564 association between SWC and microbial composition was partly shared with other soil
565 properties. Higher SWC sites may also have higher organic matter and nutrient
566 availability simultaneously, allowing microbes to respond to combined water–carbon–
567 nitrogen conditions rather than to water alone. Similar coupled environmental
568 responses have been reported in global grassland microbial studies (Leff et al., 2015).

569 An important limitation is that SWC was measured at only one time point. Soil water
570 content can vary with rainfall and drying conditions, so the single measurement
571 provides only a snapshot of soil water conditions during the sampling period. This
572 limits our ability to determine whether the observed association between SWC and
573 microbial composition would remain consistent under different hydrological conditions.
574 Repeated measurements under different hydrological conditions would help determine
575 whether the observed relationship between topography, SWC and microbial
576 composition is consistent over time.

577 ***Taxonomic and targeted functional responses were linked, but not identical***

578 The genus and targeted KO datasets showed similar overall compositional responses
579 across environmental gradients. PERMANOVA showed significant topographic effects
580 in both datasets (Table 2). VPA, however, revealed different contribution patterns
581 between taxonomic and functional composition (Figure 5; Table 3). Genus-level
582 composition showed a stronger association with soil properties, whereas targeted KO
583 composition was mainly explained by shared environmental effects. The heatmaps
584 further supported this difference (Figure 6). Top 20 Taxa associated with SWC showed
585 relatively consistent positive relationships with SWC, whereas targeted functional

genes displayed more heterogeneous abundance patterns across samples. Different microbial taxa may perform overlapping ecological functions under similar environmental conditions. Louca et al. described this phenomenon as functional redundancy, where taxonomic turnover does not necessarily produce proportional functional turnover (Louca et al., 2018). Chen et al. also reported stronger variation in microbial taxonomy than in functional profiles across soil ecosystems (Chen et al., 2022). Our β-diversity partitioning results are consistent with this interpretation. Turnover dominated β-diversity at both genus and targeted KO levels. This indicates that community differences were primarily caused by replacement among samples rather than nested loss. Baselga proposed that turnover and nestedness represent distinct ecological components of β-diversity, with turnover reflecting species replacement among habitats (Baselga, 2010b). In our study, taxonomic replacement showed stronger differentiation across local environmental heterogeneity, whereas targeted functional profiles showed stronger associations with combined environmental conditions.

Limitation and implications

Several limitations should be considered when interpreting these findings. First, the sampling design included only two independent samples for each desertification stage × topography combination. Although both topographic positions were represented across all six desertification stages, the limited replication reduces statistical power to detect local-scale differences and limits the generality of the findings. In addition, all samples were collected within a single pasture, which may not capture broader spatial variation among alpine meadow sites. Future studies should increase spatial replication within each stage × topography combination and include multiple pastures or sites. Second, SWC was measured on a single occasion, providing a snapshot of hydrological conditions rather than capturing temporal variation associated with rainfall and drying. Repeated measurements across different hydrological conditions would help determine whether the observed associations remain consistent over time. Third, parent material

and soil texture were not directly measured. Although all samples were collected within the same pasture, small-scale variation in these properties may have contributed to spatial variation in SWC and microbial composition. Finally, the strong correlations among SWC, SOM, TN, TC, and BD indicate a coupled soil physicochemical gradient. Therefore, the observed associations should not be interpreted as independent causal effects of individual soil properties.

Despite these limitations, the results highlight the importance of local environmental heterogeneity in understanding microbial variation during alpine meadow desertification. The significant topographic associations with microbial composition and the strong association of SWC with microbial composition suggest that future studies should consider local-scale environmental variation and multiple interacting soil properties rather than relying solely on categorical desertification stages. Spatially replicated sampling across multiple sites, combined with repeated measurements of SWC and soil properties, would provide stronger evidence for understanding microbial responses to desertification.

Conclusion

Topography was more strongly associated with microbial variation than the degradation stage in degraded alpine meadow soils on the QTP. SWC represented an important environmental gradient and was strongly associated with microbial composition, but its independent contribution was low after environmental partitioning. However, the strong covariance between SWC and other soil physicochemical properties indicates that its association with microbial composition should be interpreted as part of a coupled environmental gradient rather than as an isolated effect. Genus-level composition showed stronger independent associations with soil properties, whereas targeted functional composition was mainly associated with shared environmental effects. Significant topographic effects were detected for both genus-level and targeted functional composition. Turnover dominated β-diversity at both taxonomic and targeted

functional levels, indicating that microbial variation was mainly driven by habitat replacement. These findings suggest that topography-mediated environmental heterogeneity is an important factor associated with microbial taxonomic and functional organization during alpine meadow desertification.

Compliance and ethics

The authors declare that they have no conflict of interest. This study did not involve human participants, personal data, or animal experimentation. Therefore, ethical approval was not required.

Data availability

The raw sequencing data generated in this study have been deposited in the NCBI Sequence Read Archive under BioProject number PRJNA1519157. The data are available at https://dataview.ncbi.nlm.nih.gov/object/PRJNA1519157?reviewer=gup32t4lqe74p8v419rjk5oaes

Tables

Table 1 Summary statistics and environmental variable loadings of the first two principal components (PC1 and PC2) from PCA.

Variable or PCA statistic	PC1	PC2
Eigenvalue (SD)	2.577	1.279
Variance explained (%)	66.40	16.37
Cumulative variance (%)	66.40	82.77
SWC	−0.369	0.054
Bulk density	0.319	−0.096
TC	−0.384	0.037
TN	−0.380	0.097
SOM	−0.381	−0.050
pH	−0.234	0.093
DOC	−0.309	−0.414
DN	−0.173	0.592
Root biomass	−0.116	−0.667
Carbon stock	−0.362	−0.004

Note: Eigenvalues (SD), variance explained, and cumulative variance summarise the first two components. Loadings indicate the direction and relative contribution of each environmental variable to each principal component; positive and negative values indicate associations in opposite directions. Abbreviations: SWC, soil water content; TC, total carbon; TN, total nitrogen; SOM, soil organic matter; DOC, dissolved organic carbon; DN, dissolved nitrogen.

Table 2 PERMANOVA results for microbial taxonomic (Genus) and functional (KO) composition.

Dataset	Variable	Df	R^2	F	P value
Genus	Overall model	7	0.466	1.997	0.036
Genus	Degradation Stage	5	0.234	1.401	0.194
Genus	Topography	1	0.118	3.539	0.043
Genus	SWC	1	0.035	1.057	0.373
KO	Overall model	7	0.467	2.000	0.043
KO	Degradation Stage	5	0.229	1.372	0.192
KO	Topography	1	0.119	3.582	0.031
KO	SWC	1	0.035	1.053	0.360
Genus dispersion	Degradation Stage	5	—	0.592	0.706
KO dispersion	Degradation Stage	5	—	0.589	0.709

Note: Results show the effects of degradation stage, topography, and SWC on microbial composition. R^2 values indicate the proportion of variation explained by each variable. Multivariate dispersion tests (dispersion) were used to evaluate the homogeneity of within-group dispersion. $P < 0.05$ indicates statistical significance. Abbreviations: KO, KEGG Orthology; SWC, soil water content.

Table 3 Variance partitioning analysis (VPA) results for microbial taxonomic (Genus) and functional (KO) composition.

Component	KO (Adj. R^2)	Genus (Adj. R^2)
SWC	-0.019	0.013
Soil properties	-0.034	0.151
Structure (stage + topography)	0.027	0.025
Shared fractions	0.546	0.195
Residual	0.324	0.435

Total explained	0.676	0.565

Note: VPA shows the relative contributions of SWC, soil properties, and structural factors to microbial composition. Values represent adjusted R^2 fractions. Negative adjusted R^2 values indicate limited independent explanatory effects after adjustment and are not displayed in the VPA diagram. Structural factors include degradation stage and topography. Abbreviations as in Table 1 and Table 2.

Table S1 Summary of sampling design and key environmental variables across degradation stages.

Degradation Stage	Soil Water Content/%	Underground Biomass/g	pH	Bulk Density/(g/cm3)	Total Nitrogen/(mg/g)	Total Carbon/(mg/g)	Soil Organic Matter/(mg/g)	Dissolved Organic Carbon/(mg/g)	Dissolved Nitrogen/(mg/g)	Topography
1	0.343	0.549	5.730	0.684	7.037	68.178	159.698	0.726	0.239	Slope
1	0.322	0.107	5.755	0.730	6.322	59.462	167.863	0.658	0.208	Slope
2	0.311	0.080	5.890	0.585	5.451	63.982	147.293	0.658	0.245	Slope
2	0.346	0.678	5.870	0.661	6.363	72.197	159.612	0.807	0.298	Slope
3	0.351	0.150	5.825	0.685	5.256	61.852	144.979	0.570	0.194	Slope
3	0.376	0.240	5.855	0.722	5.886	69.639	147.875	0.659	0.247	Slope
4	0.328	0.025	5.975	0.760	4.733	51.522	108.461	0.464	0.173	Slope

4	0.303	0.056	6.095	0.869	4.570	52.637	106.329	0.437	0.122	Slope
5	0.327	0.149	6.560	0.678	4.806	55.247	121.810	0.557	0.176	Slope
5	0.361	0.380	5.970	0.540	5.783	68.361	154.271	0.617	0.193	Slope
6	0.270	0.010	6.440	0.888	4.835	51.973	113.794	0.527	0.113	Slope
6	0.283	0.049	6.075	0.691	5.532	51.468	109.759	0.545	0.220	Slope
1	0.560	0.384	6.440	0.477	16.173	193.251	418.182	1.385	0.305	Flatplain
1	0.490	0.908	7.030	0.534	10.965	128.862	300.470	1.265	0.218	Flatplain
2	0.497	0.162	6.490	0.516	10.727	123.759	254.526	0.936	0.225	Flatplain
2	0.579	0.220	6.620	0.287	18.118	213.251	405.975	3.232	0.298	Flatplain
3	0.425	0.666	6.765	0.569	9.424	106.440	267.983	0.834	0.215	Flatplain

3	0.472	0.074	7.095	0.580	9.794	112.468	261.162	0.538	0.390	Flatplain
4	0.522	0.050	6.265	0.445	12.372	139.315	258.622	1.583	0.831	Flatplain
4	0.483	0.044	6.675	0.493	10.805	117.675	228.119	0.692	0.497	Flatplain
5	0.397	0.011	6.315	0.511	10.136	105.364	233.427	0.696	0.678	Flatplain
5	0.440	0.009	6.345	0.560	9.228	100.489	206.812	0.623	0.691	Flatplain
6	0.479	0.011	6.550	0.513	11.812	127.055	265.241	0.705	0.675	Flatplain
6	0.267	0.024	6.430	0.823	6.353	58.149	142.932	0.471	0.579	Flatplain

Note: Degradation stages are coded 1–6. Abbreviations: SWC, soil water content; TN, total nitrogen; TC, total carbon; SOM, soil organic matter; DOC, dissolved organic carbon; DN, dissolved nitrogen.

Table S2 Pearson correlation coefficients (r) among soil water content (SWC) and soil physicochemical properties.

Variable	SWC	SOM	TN	TC	pH	Bulk Density
SWC	1.000	0.923***	0.931***	0.947***	0.561**	−0.872***
SOM	0.923***	1.000	0.970***	0.978***	0.578**	−0.821***
TN	0.931***	0.970***	1.000	0.991***	0.543**	−0.848***
TC	0.947***	0.978***	0.991***	1.000	0.546**	−0.853***
pH	0.561**	0.578**	0.543**	0.546**	1.000	−0.403
Bulk Density	−0.872***	−0.821***	−0.848***	−0.853***	−0.403	1.000

Note: P < 0.05; *P < 0.01; **P < 0.001. Abbreviations as in Table S1.

Table S3 Two-way analysis of variance (ANOVA) testing the effects of degradation stage, topographic position, and their interaction on soil water content (SWC).

Source	df	F	P
Degradation stage	5	2.34	0.106
Topographic position	1	43.17	<0.001
Degradation stage × Topographic position	5	1.37	0.302
Residuals	12	—	—

Note: Degrees of freedom (df), F-statistic, and P-values are shown.

Table S4 Environmental fitting results for genus-level microbial community composition based on NMDS ordination.

Variable	NMDS1	NMDS2	r^2	P value
SWC	0.508	0.861	0.644	0.001
SOM	0.428	0.904	0.677	0.001

TN	0.359	0.934	0.703	0.001
TC	0.383	0.924	0.684	0.001
pH	0.672	0.741	0.591	0.001
BD	−0.486	−0.874	0.508	0.001

Note: Coordinates indicate vector directions on the NMDS axes. r^2 values represent the strength of associations between environmental variables and microbial community composition. Abbreviations as in Table S1 and Table 1.

Table S5 Overall distance-based redundancy analysis (dbRDA) model statistics and permutation tests for microbial functional (KO) and taxonomic (Genus) composition.

Statistic / variable	**KO**	**Genus**
Total inertia	0.005785	0.017984
Constrained inertia	0.002288	0.007229
Unconstrained inertia	0.003497	0.010755
R^2	0.3955	0.4020
Adjusted R^2	0.3049	0.3123
Overall model F	4.3623	4.4813
Overall model P	0.002	0.001
SWC F	9.38	9.88
SWC P	0.002**	0.001***
SOM F	0.75	1.58
SOM P	0.498 ns	0.190 ns
TN F	2.96	1.98
TN P	0.043*	0.127 ns

Note: Total inertia represents total community variation; constrained inertia represents variation explained by the environmental variables; unconstrained inertia represents residual variation.

R^2 and adjusted R^2 indicate the proportion of variation explained by the model. $P < 0.05$; *$P < 0.01$; **$P < 0.001$; ns, not significant. Abbreviations as in Table 1 and Table 2.

Table S6 Linear regression results testing the relationships between SWC distance and turnover or nestedness components of microbial β-diversity.

Model	**R^2**	**P value**
Genus turnover	0.0027	0.391
Genus nestedness	0.0264	0.0069
KO turnover	0.0048	0.253
KO nestedness	0.0003	0.763

Note: R^2 values indicate model explanatory power, and P-values indicate statistical significance. Abbreviations: SWC, soil water content; KO, KEGG Orthology.

Figures

Figure 1 Geographic distribution of sampling sites in degraded alpine meadows on the QTP. Sampling locations were classified into two topographic types: slope (red circles, left panel region) and flatplain (yellow circles, right panel region). A total of 24 sampling sites were included for subsequent analyses. Background imagery represents the landscape characteristics of the study area, and coordinates indicate the geographic position of each sampling site.

Figure 2 (A) Principal component analysis (PCA) of soil environmental variables across six degradation stages and two topographic positions. PC1 and PC2 explain 72.3% and 11.7% of the total variation, respectively. Symbols indicate topographic positions, and colours represent degradation stages. (B, C) Soil water content (SWC) across six degradation stages (B) and between flatplain and slope habitats (C) Boxplots show medians, interquartile ranges (IQRs), and whiskers extending to 1.5 × IQR; points represent individual observations. Differences among degradation stages were assessed using the Kruskal–Wallis test, and differences between topographic positions using the Wilcoxon rank-sum test. Asterisks indicate statistical significance (*P < 0.05, **P < 0.01, ***P < 0.001).

Figure 3 NMDS ordination of genus-level microbial community composition with environmental fitting. Colors indicate degradation stages and symbols represent topographic categories (circles: flatplain; triangles: slope). Ellipses indicate group distributions within degradation stages. Environmental vectors were fitted using the envfit procedure, and arrow lengths indicate the relative strength of associations between environmental variables and microbial community composition. The stress value indicates the goodness-of-fit of the two-dimensional ordination.

Figure 4 dbRDA of microbial taxonomic and functional composition. (A) Genus-level taxonomic composition. (B) KO functional composition. Arrows indicate the direction

and magnitude of environmental gradients, including SWC, SOM, and TN. The percentage explained by each axis is shown in parentheses. Sample colors indicate soil water content gradients.

Figure 5 VPA of microbial taxonomic and functional composition. VPA showing the relative contributions of SWC, soil properties, and structural factors (degradation stage + topography) to genus-level microbial composition (A) and targeted functional composition (B). Values indicate adjusted R^2 fractions attributed to unique and shared contributions of environmental components. Negative adjusted R^2 values are not displayed.

Figure 6 (A) SWC-associated microbial taxa across environmental gradients. Heatmap showing the top 20 microbial taxa associated with SWC. Samples are ordered by SWC and annotated by topographic position, degradation stage, and SWC. Taxa were selected based on Spearman correlations with SWC. Spearman rho and FDR values are shown beside each taxon. Abundance values were standardized by z-score transformation. (B) Targeted functional genes across environmental gradients. Heatmap showing targeted functional genes related to carbon cycling, nitrogen cycling, stress resistance, and other selected ecological functions. Samples are annotated by topographic position, degradation stage, and SWC. Genes are annotated by functional category. Abundance values were standardized by z-score transformation.

Figure S1 Genus-level microbial alpha diversity across degradation stages. (A) Shannon diversity index, (B) richness, and (C) Simpson diversity index. Boxes represent the IQR, horizontal lines indicate median values, whiskers indicate 1.5 × IQR, and points represent individual samples. Statistical differences among degradation stages were evaluated using the Kruskal–Wallis test.

Figure S2 Turnover and nestedness components of microbial taxonomic and targeted functional β-diversity. (A–B) Relationships between SWC distance and genus-level

turnover and nestedness. (C) Genus-level turnover patterns across topographic pairwise groups. (D–E) Relationships between SWC distance and KO-level turnover and nestedness. (F) KO-level turnover patterns across topographic pairwise groups. (G) Mean effect sizes of turnover and nestedness components at genus and KO levels. (H) Model fit values (R^2) for regressions between SWC distance and β-diversity components. Shaded areas indicate 95% confidence intervals.

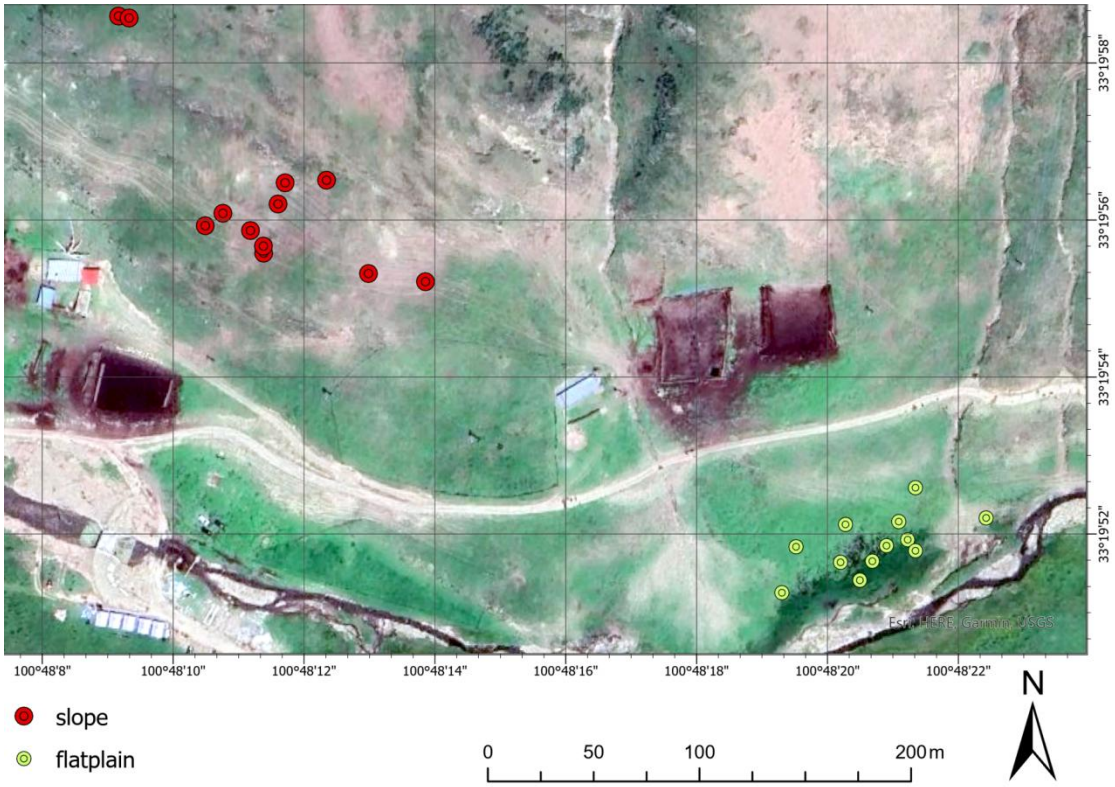

33°19'58"
33°19'56"
33°19'54"
33°19'52"
100°48'8"
100°48'10"
100°48'12"
100°48'14"
100°48'16"
100°48'18"
100°48'20"
100°48'22"
Esri, HERE, Garmin, USGS
N
slope
flatplain
0
50
100
200 m

Figure 1

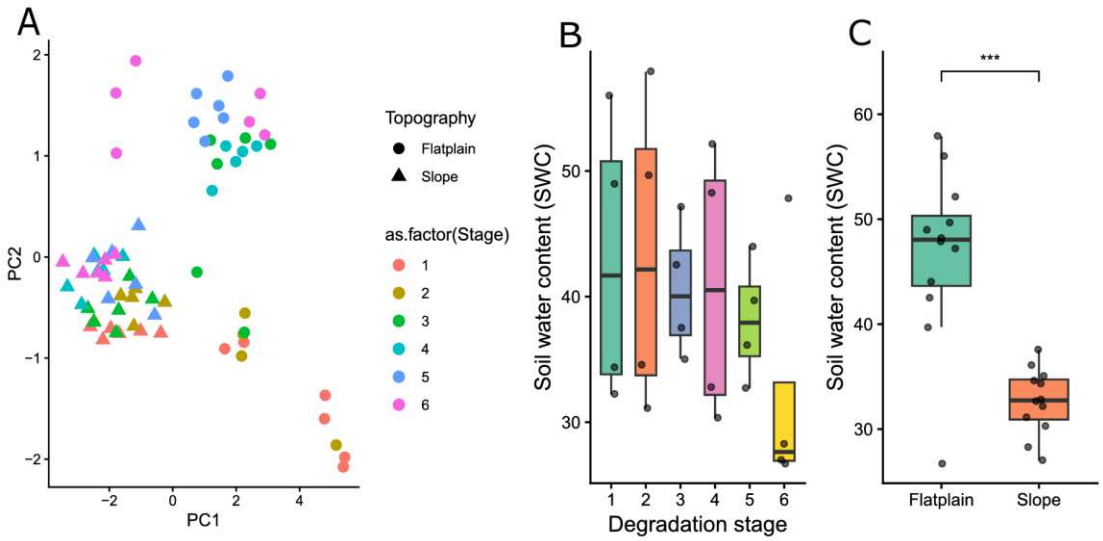

A
PC2
PC1
Topography
Flatplain
Slope
as.factor(Stage)
1
2
3
4
5
6
B
Soil water content (SWC)
Degradation stage
C
Soil water content (SWC)
***
Flatplain
Slope

Figure 2

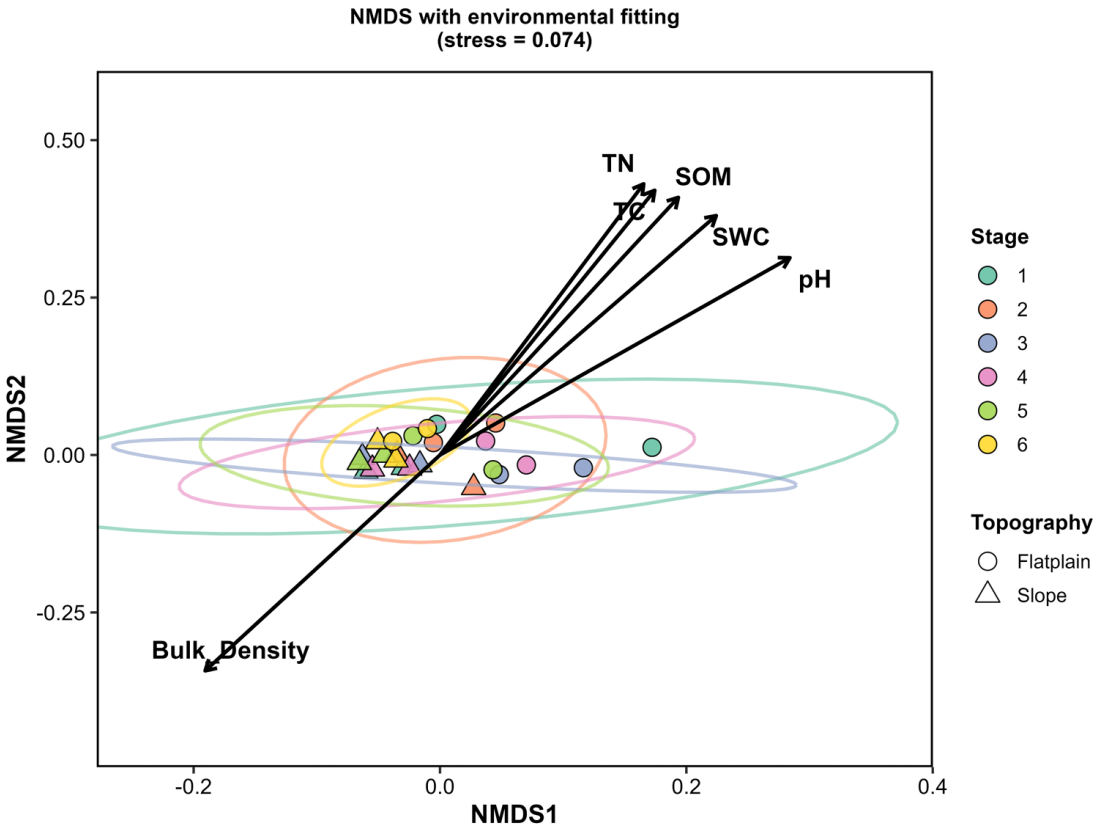

NMDS with environmental fitting
(stress = 0.074)
TN
SOM
TC
SWC
pH
Bulk_Density
NMDS1
NMDS2
0.50
0.25
0.00
-0.25
-0.2
0.0
0.2
0.4
Stage
1
2
3
4
5
6
Topography
Flatplain
Slope

Figure 3

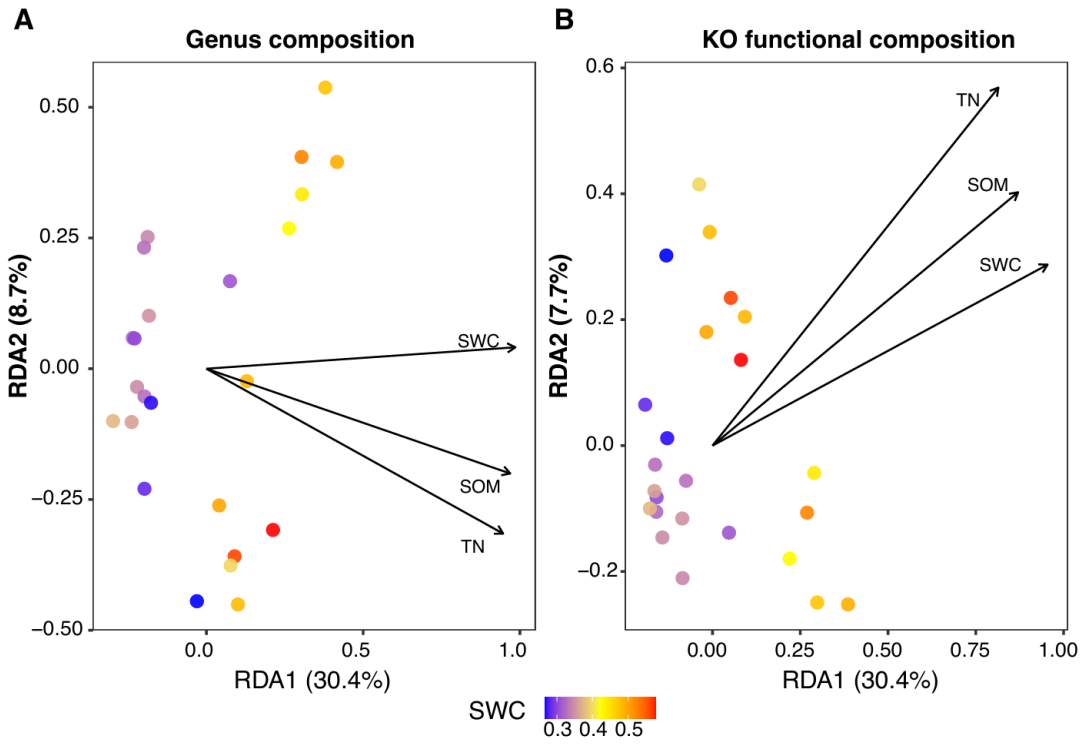

A
Genus composition
RDA2 (8.7%)
RDA1 (30.4%)
SWC
SOM
TN
B
KO functional composition
RDA2 (7.7%)
RDA1 (30.4%)
TN
SOM
SWC
SWC
0.3 0.4 0.5

Figure 4

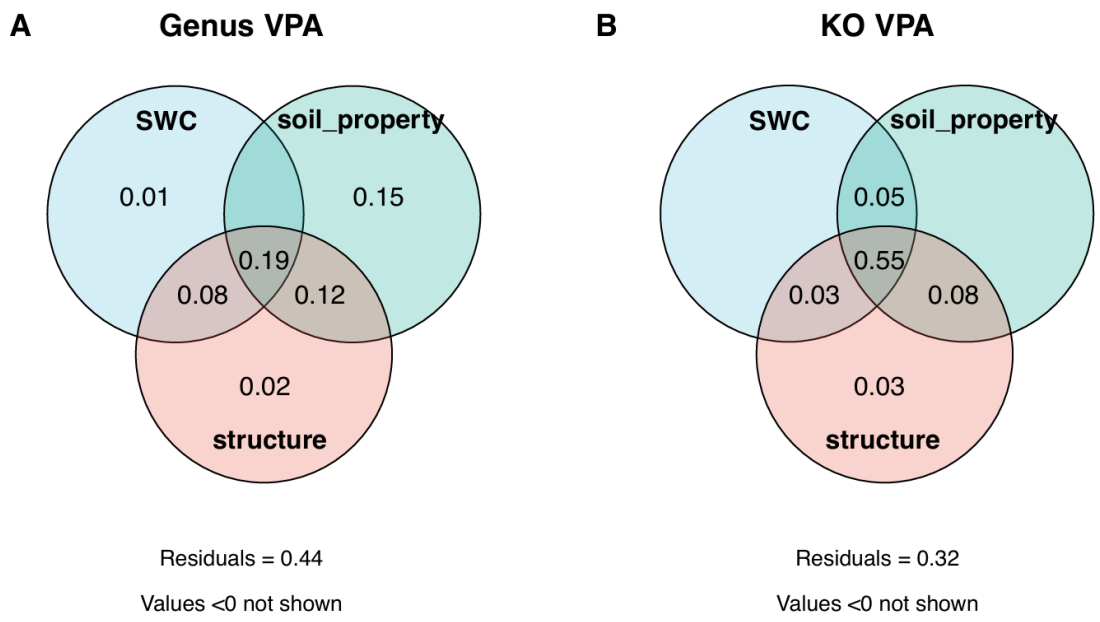

A
Genus VPA
SWC
soil_property
0.01
0.15
0.19
0.08
0.12
0.02
structure
Residuals = 0.44
Values <0 not shown
B
KO VPA
SWC
soil_property
0.05
0.55
0.03
0.08
0.03
structure
Residuals = 0.32
Values <0 not shown

Figure 5

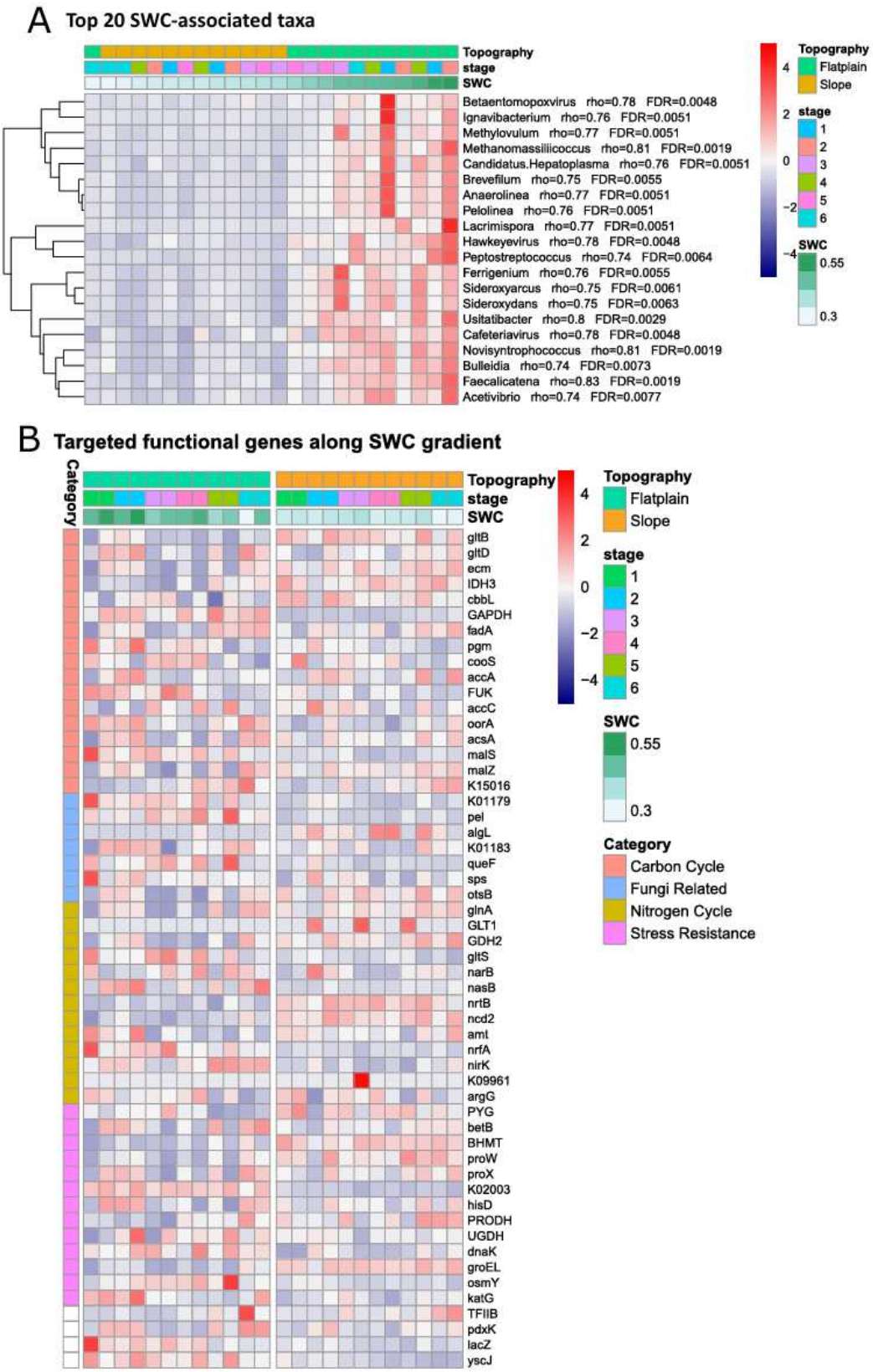

A Top 20 SWC-associated taxa
Topography
stage
SWC
Betaentomopoxvirus rho=0.78 FDR=0.0048
Ignavibacterium rho=0.76 FDR=0.0051
Methylovulum rho=0.77 FDR=0.0051
Methanomassiliicoccus rho=0.81 FDR=0.0019
Candidatus.Hepatoplasma rho=0.76 FDR=0.0051
Brevefilum rho=0.75 FDR=0.0055
Anaerolinea rho=0.77 FDR=0.0051
Pelolinea rho=0.76 FDR=0.0051
Lacrimispora rho=0.77 FDR=0.0051
Hawkeyevirus rho=0.78 FDR=0.0048
Peptostreptococcus rho=0.74 FDR=0.0064
Ferrigenium rho=0.76 FDR=0.0055
Sideroxyarcus rho=0.75 FDR=0.0061
Sideroxydans rho=0.75 FDR=0.0063
Usitatibacter rho=0.8 FDR=0.0029
Cafeteriavirus rho=0.78 FDR=0.0048
Novisyntrophococcus rho=0.81 FDR=0.0019
Bulleidia rho=0.74 FDR=0.0073
Faecalicatena rho=0.83 FDR=0.0019
Acetivibrio rho=0.74 FDR=0.0077
Topography
Flatplain
Slope
stage
1
2
3
4
5
6
SWC
0.55
0.3
B Targeted functional genes along SWC gradient
Category
gltB
gltD
ecm
IDH3
cbbL
GAPDH
fadA
pgm
cooS
accA
FUK
accC
oorA
acsA
malS
malZ
K15016
K01179
pel
algL
K01183
queF
sps
otsB
glnA
GLT1
GDH2
gltS
narB
nasB
nrtB
ncd2
amt
nrfA
nirK
K09961
argG
PYG
betB
BHMT
proW
proX
K02003
hisD
PRODH
UGDH
dnaK
groEL
osmY
katG
TFIIB
pdxK
lacZ
yscJ
Category
Carbon Cycle
Fungi Related
Nitrogen Cycle
Stress Resistance

Figure 6

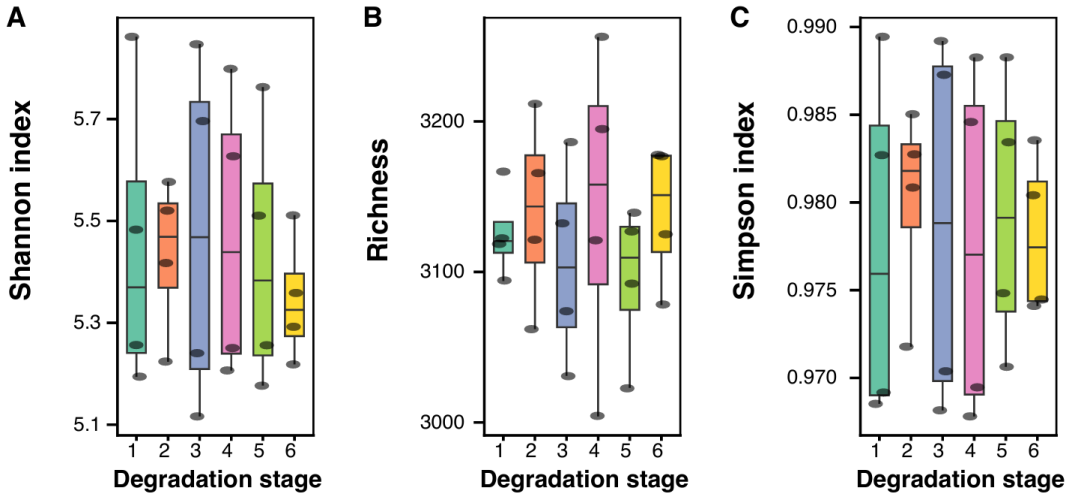

A
Shannon index
5.7
5.5
5.3
5.1
1 2 3 4 5 6
Degradation stage
B
Richness
3200
3100
3000
1 2 3 4 5 6
Degradation stage
C
Simpson index
0.990
0.985
0.980
0.975
0.970
1 2 3 4 5 6
Degradation stage

Figure S1

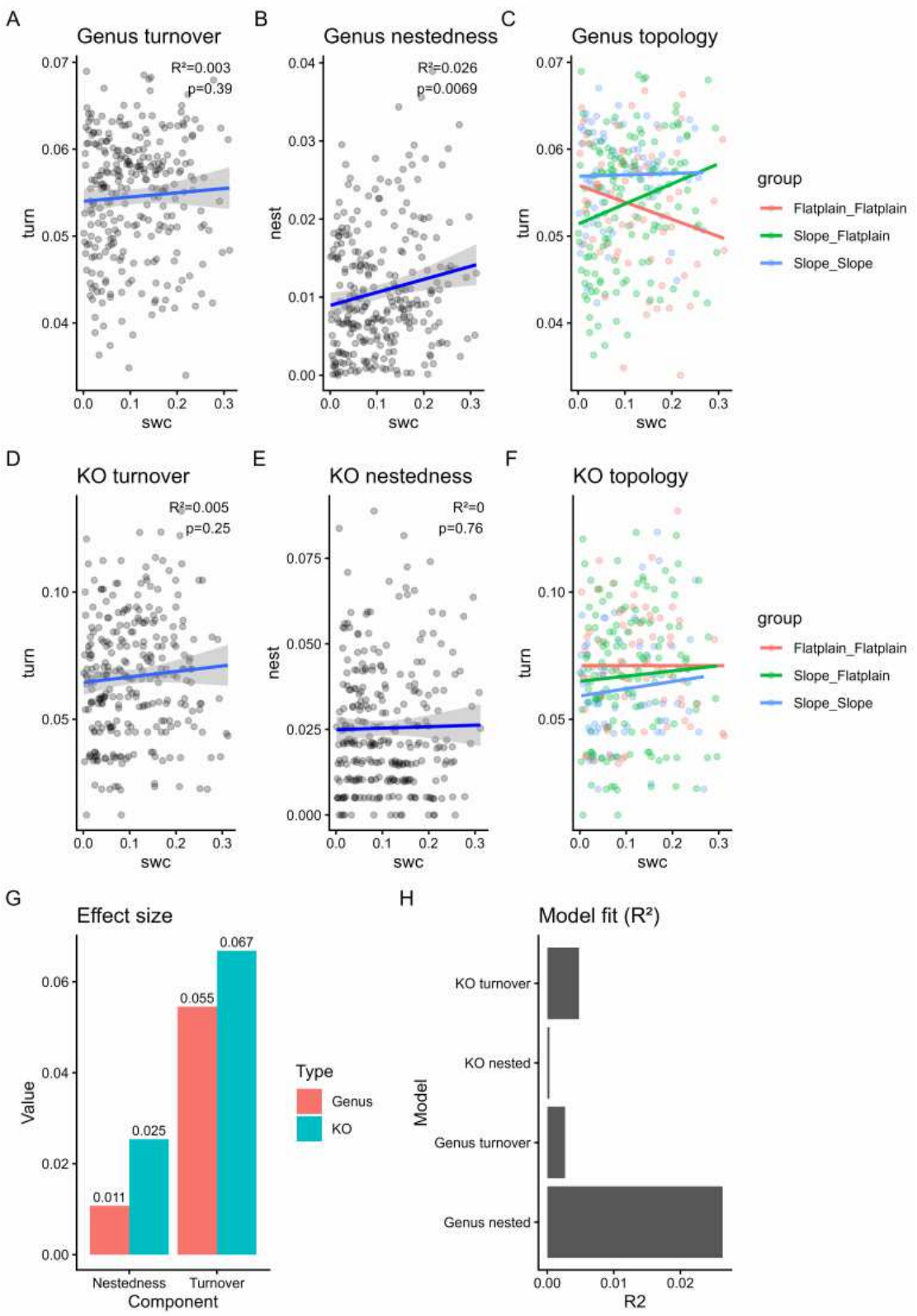

A
Genus turnover
R²=0.003
p=0.39
turn
swc
B
Genus nestedness
R²=0.026
p=0.0069
nest
swc
C
Genus topology
turn
swc
group
Flatplain_Flatplain
Slope_Flatplain
Slope_Slope
D
KO turnover
R²=0.005
p=0.25
turn
swc
E
KO nestedness
R²=0
p=0.76
nest
swc
F
KO topology
turn
swc
group
Flatplain_Flatplain
Slope_Flatplain
Slope_Slope
G
Effect size
Value
0.011
0.025
0.055
0.067
Nestedness
Turnover
Component
Type
Genus
KO
H
Model fit (R²)
KO turnover
KO nested
Genus turnover
Genus nested
Model
R2

Figure S2

References

Anderson, M.J., 2001. A new method for non-parametric multivariate analysis of variance. Austral Ecology 26, 32–46. https://doi.org/10.1111/j.1442-9993.2001.01070.pp.x

Anderson, M.J., Crist, T.O., Chase, J.M., Vellend, M., Inouye, B.D., Freestone, A.L., Sanders, N.J., Cornell, H.V., Comita, L.S., Davies, K.F., Harrison, S.P., Kraft, N.J.B., Stegen, J.C., Swenson, N.G., 2011. Navigating the multiple meanings of β diversity: a roadmap for the practicing ecologist: Roadmap for beta diversity. Ecology Letters 14, 19–28. https://doi.org/10.1111/j.1461-0248.2010.01552.x

Banerjee, S., Helgason, B., Wang, L., Winsley, T., Ferrari, B.C., Siciliano, S.D., 2016. Legacy effects of soil moisture on microbial community structure and N2O emissions. Soil Biology and Biochemistry 95, 40–50. https://doi.org/10.1016/j.soilbio.2015.12.004

Bardgett, R.D., Van Der Putten, W.H., 2014. Belowground biodiversity and ecosystem functioning. Nature 515, 505–511. https://doi.org/10.1038/nature13855

Baselga, A., 2013. Separating the two components of abundance-based dissimilarity: balanced changes in abundance vs. abundance gradients. Methods Ecol Evol 4, 552–557. https://doi.org/10.1111/2041-210X.12029

Baselga, A., 2010a. Partitioning the turnover and nestedness components of beta diversity. Global Ecology and Biogeography 19, 134–143. https://doi.org/10.1111/j.1466-8238.2009.00490.x

Baselga, A., 2010b. Partitioning the turnover and nestedness components of beta diversity. Global Ecology and Biogeography 19, 134–143. https://doi.org/10.1111/j.1466-8238.2009.00490.x

Beghini, F., McIver, L.J., Blanco-Míguez, A., Dubois, L., Asnicar, F., Maharjan, S., Mailyan, A., Manghi, P., Scholz, M., Thomas, A.M., Valles-Colomer, M., Weingart, G., Zhang, Y., Zolfo, M., Huttenhower, C., Franzosa, E.A., Segata, N., 2021. Integrating taxonomic, functional, and strain-level profiling of diverse microbial communities with bioBakery 3. eLife 10, e65088. https://doi.org/10.7554/eLife.65088

Benjamini, Y., Hochberg, Y., 1995. Controlling the False Discovery Rate: A Practical and Powerful Approach to Multiple Testing. Journal of the Royal Statistical Society Series B: Statistical Methodology 57, 289–300. https://doi.org/10.1111/j.2517-6161.1995.tb02031.x

Berdugo, M., Delgado-Baquerizo, M., Soliveres, S., Hernández-Clemente, R., Zhao, Y., Gaitán, J.J., Gross, N., Saiz, H., Maire, V., Lehmann, A., Rillig, M.C., Solé, R.V., Maestre, F.T.,

2020. Global ecosystem thresholds driven by aridity. Science 367, 787–790. https://doi.org/10.1126/science.aay5958

Bowd, E.J., Banks, S.C., Strong, C.L., Lindenmayer, D.B., 2019. Long-term impacts of wildfire and logging on forest soils. Nature Geosci 12, 113–118. https://doi.org/10.1038/s41561-018-0294-2

Breshears, D.D., Cobb, N.S., Rich, P.M., Price, K.P., Allen, C.D., Balice, R.G., Romme, W.H., Kastens, J.H., Floyd, M.L., Belnap, J., Anderson, J.J., Myers, O.B., Meyer, C.W., 2005. Regional vegetation die-off in response to global-change-type drought. Proc. Natl. Acad. Sci. U.S.A. 102, 15144–15148. https://doi.org/10.1073/pnas.0505734102

Brockett, B.F.T., Prescott, C.E., Grayston, S.J., 2012. Soil moisture is the major factor influencing microbial community structure and enzyme activities across seven biogeoclimatic zones in western Canada. Soil Biology and Biochemistry 44, 9–20. https://doi.org/10.1016/j.soilbio.2011.09.003

Canarini, A., Schmidt, H., Fuchslueger, L., Martin, V., Herbold, C.W., Zezula, D., Gündler, P., Hasibeder, R., Jecmenica, M., Bahn, M., Richter, A., 2021. Ecological memory of recurrent drought modifies soil processes via changes in soil microbial community. Nat Commun 12, 5308. https://doi.org/10.1038/s41467-021-25675-4

Chapin Iii, F.S., Zavaleta, E.S., Eviner, V.T., Naylor, R.L., Vitousek, P.M., Reynolds, H.L., Hooper, D.U., Lavorel, S., Sala, O.E., Hobbie, S.E., Mack, M.C., Díaz, S., 2000. Consequences of changing biodiversity. Nature 405, 234–242. https://doi.org/10.1038/35012241

Chen, Huaihai, Ma, K., Lu, C., Fu, Q., Qiu, Y., Zhao, J., Huang, Y., Yang, Y., Schadt, C.W., Chen, Hao, 2022. Functional Redundancy in Soil Microbial Community Based on Metagenomics Across the Globe. Front. Microbiol. 13, 878978. https://doi.org/10.3389/fmicb.2022.878978

Dai, L., Fu, R., Guo, X., Du, Y., Zhang, F., Cao, G., 2023. Variations in and factors controlling soil hydrological properties across different slope aspects in alpine meadows. Journal of Hydrology 616, 128756. https://doi.org/10.1016/j.jhydrol.2022.128756

Delaux, P.-M., Séjalon-Delmas, N., Bécard, G., Ané, J.-M., 2013. Evolution of the plant–microbe symbiotic 'toolkit.' Trends in Plant Science 18, 298–304. https://doi.org/10.1016/j.tplants.2013.01.008

D'Odorico, P., Bhattachan, A., Davis, K.F., Ravi, S., Runyan, C.W., 2013. Global desertification: Drivers and feedbacks. Advances in Water Resources 51, 326–344. https://doi.org/10.1016/j.advwatres.2012.01.013

Dong, S., Zhang, Y., Shen, H., Li, S., Xu, Y., 2023. Future of the Third Pole's Grasslands, in: Grasslands on the Third Pole of the World. Springer International Publishing, Cham, pp. 347–353. https://doi.org/10.1007/978-3-031-39485-0_11

Dunn, O.J., 1964. Multiple Comparisons Using Rank Sums. Technometrics 6, 241–252. https://doi.org/10.1080/00401706.1964.10490181

Ellis, E.C., 2011. Anthropogenic transformation of the terrestrial biosphere. Phil. Trans. R. Soc. A. 369, 1010–1035. https://doi.org/10.1098/rsta.2010.0331

Fierer, N., 2017. Embracing the unknown: disentangling the complexities of the soil microbiome. Nat Rev Microbiol 15, 579–590. https://doi.org/10.1038/nrmicro.2017.87

Fierer, N., Jackson, R.B., 2006. The diversity and biogeography of soil bacterial communities. Proc. Natl. Acad. Sci. U.S.A. 103, 626–631. https://doi.org/10.1073/pnas.0507535103

Ghabbour, E.A., Davies, G., Cuozzo, N.P., Miller, R.O., 2014. Optimized conditions for determination of total soil organic matter in diverse samples by mass loss on ignition. J. Plant Nutr. Soil Sci. 177, 914–919. https://doi.org/10.1002/jpln.201400326

Han, Y., 2015. Analysis of Climate Change in Jiu Zhi County over the Past 49 Years.

Harris, R.B., 2010. Rangeland degradation on the Qinghai-Tibetan plateau: A review of the evidence of its magnitude and causes. Journal of Arid Environments 74, 1–12. https://doi.org/10.1016/j.jaridenv.2009.06.014

Intergovernmental Panel On Climate Change (Ipcc), 2023. Climate Change 2021 – The Physical Science Basis: Working Group I Contribution to the Sixth Assessment Report of the Intergovernmental Panel on Climate Change, 1st ed. Cambridge University Press. https://doi.org/10.1017/9781009157896

Kanehisa, M., 2000. KEGG: Kyoto Encyclopedia of Genes and Genomes. Nucleic Acids Research 28, 27–30. https://doi.org/10.1093/nar/28.1.27

Knapp, A.K., Beier, C., Briske, D.D., Classen, A.T., Luo, Y., Reichstein, M., Smith, M.D., Smith, S.D., Bell, J.E., Fay, P.A., Heisler, J.L., Leavitt, S.W., Sherry, R., Smith, B., Weng, E., 2008. Consequences of More Extreme Precipitation Regimes for Terrestrial Ecosystems. BioScience 58, 811–821. https://doi.org/10.1641/B580908

Kolde, R., 2010. pheatmap: Pretty Heatmaps. https://doi.org/10.32614/CRAN.package.pheatmap

Kruskal, W.H., Wallis, W.A., 1952. Use of Ranks in One-Criterion Variance Analysis. Journal of the American Statistical Association 47, 583–621.

https://doi.org/10.1080/01621459.1952.10483441

Leff, J.W., Jones, S.E., Prober, S.M., Barberán, A., Borer, E.T., Firn, J.L., Harpole, W.S., Hobbie, S.E., Hofmockel, K.S., Knops, J.M.H., McCulley, R.L., La Pierre, K., Risch, A.C., Seabloom, E.W., Schütz, M., Steenbock, C., Stevens, C.J., Fierer, N., 2015. Consistent responses of soil microbial communities to elevated nutrient inputs in grasslands across the globe. Proc. Natl. Acad. Sci. U.S.A. 112, 10967–10972. https://doi.org/10.1073/pnas.1508382112

Legendre, P., 2008. Studying beta diversity: ecological variation partitioning by multiple regression and canonical analysis. Journal of Plant Ecology 1, 3–8. https://doi.org/10.1093/jpe/rtm001

Legendre, P., Anderson, M.J., 1999. DISTANCE-BASED REDUNDANCY ANALYSIS: TESTING MULTISPECIES RESPONSES IN MULTIFACTORIAL ECOLOGICAL EXPERIMENTS. Ecological Monographs 69, 1–24. https://doi.org/10.1890/0012-9615(1999)069[0001:DBRATM]2.0.CO;2

Legendre, P., De Cáceres, M., 2013. Beta diversity as the variance of community data: dissimilarity coefficients and partitioning. Ecology Letters 16, 951–963. https://doi.org/10.1111/ele.12141

Li, L., Fassnacht, F.E., Storch, I., Bürgi, M., 2017. Land-use regime shift triggered the recent degradation of alpine pastures in Nyanpo Yutse of the eastern Qinghai-Tibetan Plateau. Landscape Ecol 32, 2187–2203. https://doi.org/10.1007/s10980-017-0510-2

Li, Xinwei, Li, Xilai, Shi, Y., Zhao, S., Liu, J., Lin, Y., Li, C., Zhang, C., 2024. Effects of microtopography on soil microbial communities in alpine meadows on the Qinghai-Tibetan Plateau. CATENA 239, 107945. https://doi.org/10.1016/j.catena.2024.107945

Louca, S., Polz, M.F., Mazel, F., Albright, M.B.N., Huber, J.A., O'Connor, M.I., Ackermann, M., Hahn, A.S., Srivastava, D.S., Crowe, S.A., Doebeli, M., Parfrey, L.W., 2018. Function and functional redundancy in microbial systems. Nat Ecol Evol 2, 936–943. https://doi.org/10.1038/s41559-018-0519-1

Miehe, G., Schleuss, P.-M., Seeber, E., Babel, W., Biermann, T., Braendle, M., Chen, F., Coners, H., Foken, T., Gerken, T., Graf, H.-F., Guggenberger, G., Hafner, S., Holzapfel, M., Ingrisch, J., Kuzyakov, Y., Lai, Z., Lehnert, L., Leuschner, C., Li, X., Liu, J., Liu, S., Ma, Y., Miehe, S., Mosbrugger, V., Noltie, H.J., Schmidt, J., Spielvogel, S., Unteregelsbacher, S., Wang, Y., Willinghöfer, S., Xu, X., Yang, Y., Zhang, S., Opgenoorth, L., Wesche, K., 2019. The Kobresia pygmaea ecosystem of the Tibetan highlands - Origin, functioning and degradation of the world's largest pastoral alpine ecosystem: Kobresia pastures of Tibet. Sci Total Environ 648, 754–771.

https://doi.org/10.1016/j.scitotenv.2018.08.164

Oksanen, J., Simpson, G.L., Blanchet, F.G., Kindt, R., Legendre, P., Minchin, P.R., O'Hara, R.B., Solymos, P., Stevens, M.H.H., Szoecs, E., Wagner, H., Barbour, M., Bedward, M., Bolker, B., Borcard, D., Borman, T., Carvalho, G., Chirico, M., De Caceres, M., Durand, S., Evangelista, H.B.A., FitzJohn, R., Friendly, M., Furneaux, B., Hannigan, G., Hill, M.O., Lahti, L., Martino, C., McGlinn, D., Ouellette, M.-H., Ribeiro Cunha, E., Smith, T., Stier, A., Ter Braak, C.J.F., Weedon, J., 2001. vegan: Community Ecology Package. https://doi.org/10.32614/CRAN.package.vegan

Qian, J., Wang, D., Zhao, L., Cui, Z., Li, S., Liu, Y., 2024. Severe degradation and artificial restoration diversely drive runoff and sediment processes in alpine meadows. Geoderma 443, 116828. https://doi.org/10.1016/j.geoderma.2024.116828

Schimel, J.P., 2018. Life in Dry Soils: Effects of Drought on Soil Microbial Communities and Processes. Annu. Rev. Ecol. Evol. Syst. 49, 409–432. https://doi.org/10.1146/annurev-ecolsys-110617-062614

Schuur, E.A.G., McGuire, A.D., Schädel, C., Grosse, G., Harden, J.W., Hayes, D.J., Hugelius, G., Koven, C.D., Kuhry, P., Lawrence, D.M., Natali, S.M., Olefeldt, D., Romanovsky, V.E., Schaefer, K., Turetsky, M.R., Treat, C.C., Vonk, J.E., 2015. Climate change and the permafrost carbon feedback. Nature 520, 171–179. https://doi.org/10.1038/nature14338

Sokol, N.W., Slessarev, E., Marschmann, G.L., Nicolas, A., Blazewicz, S.J., Brodie, E.L., Firestone, M.K., Foley, M.M., Hestrin, R., Hungate, B.A., Koch, B.J., Stone, B.W., Sullivan, M.B., Zablocki, O., LLNL Soil Microbiome Consortium, Trubl, G., McFarlane, K., Stuart, R., Nuccio, E., Weber, P., Jiao, Y., Zavarin, M., Kimbrel, J., Morrison, K., Adhikari, D., Bhattacharaya, A., Nico, P., Tang, J., Didonato, N., Paša-Tolić, L., Greenlon, A., Sieradzki, E.T., Dijkstra, P., Schwartz, E., Sachdeva, R., Banfield, J., Pett-Ridge, J., 2022. Life and death in the soil microbiome: how ecological processes influence biogeochemistry. Nat Rev Microbiol 20, 415–430. https://doi.org/10.1038/s41579-022-00695-z

Tecon, R., Or, D., 2017. Biophysical processes supporting the diversity of microbial life in soil. FEMS Microbiology Reviews 41, 599–623. https://doi.org/10.1093/femsre/fux039

Tian, Y., Ouyang, H., Xu, X., Song, M., Zhou, C., 2008. DISTRIBUTION CHARACTERISTICS OF SOIL ORGANIC CARBON STORAGE AND DENSITY ON THE QINGHAI-TIBET PLATEAU. Acta Pedologica Sinica 45, 933–942.

Wilcoxon, F., 1945. Individual Comparisons by Ranking Methods. Biometrics Bulletin 1, 80. https://doi.org/10.2307/3001968

Wood, D.E., Lu, J., Langmead, B., 2019. Improved metagenomic analysis with Kraken 2. Genome Biol 20, 257. https://doi.org/10.1186/s13059-019-1891-0

Wu, Y., Yang, W., Li, Q., Qiao, Q., Zhao, S., Zhang, Y., Yu, Y., Zhang, S., Li, X., Kou, J., 2024. Microbial Community Response to Alpine Meadow Degradation and Its Impact on Soil Nutrient Cycling. Agronomy 14, 195. https://doi.org/10.3390/agronomy14010195

Xue, R., Yang, Q., Miao, F., Wang, X., Shen, Y., 2018. Slope aspect influences plant biomass, soil properties and microbial composition in alpine meadow on the Qinghai-Tibetan plateau. J. Soil Sci. Plant Nutr. 0–0. https://doi.org/10.4067/S0718-95162018005000101

Yang, C., Zhang, H., Zhao, X., Liu, P., Wang, L., Wang, W., 2023. A functional metagenomics study of soil carbon and nitrogen degradation networks and limiting factors on the Tibetan plateau. Front. Microbiol. 14, 1170806. https://doi.org/10.3389/fmicb.2023.1170806

Zhang, W., Yi, S., Qin, Y., Zhang, J., 2024. Effects of Patchiness on Soil Properties and Degradation of Alpine Meadow on the Qinghai–Tibetan Plateau. Land 13, 1556. https://doi.org/10.3390/land13101556